On the cyclic behavior of wave-driven sandspits with implications for coastal zone management

Adélaïde Taveneau, Rafael Almar, Erwin W. J. Bergsma

Estuarine, Coastal and Shelf Science 303 (2024) 108798

Contents lists available at ScienceDirect

Estuarine, Coastal and Shelf Science

journal homepage: www.elsevier.com/locate/ecss

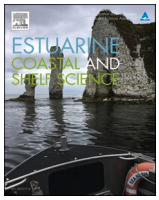

On the cyclic behavior of wave-driven sandspits with implications for coastal zone management

Adélaïde Taveneau [a,*], Rafael Almar [a], Erwin W.J. Bergsma [b]

[a] Institut de Recherche pour le Développement, LEGOS (IRD/CNES/Université de Toulouse), 31400, Toulouse, France
[b] Centre National D'Etudes Spatiales (CNES), 31400, Toulouse, France

ARTICLE INFO

Keywords:
Sandspit behavior
Satellite images
Conceptual model
Cyclic

ABSTRACT

Sandspits at river mouths are important socio-ecological but fragile coastal ecosystems. Due to their significant role, particularly in shielding areas behind them from wave impact, sandspits are crucial, albeit they also pose challenges such as increased fluvial flooding, which often necessitates substantial engineering interventions such as artificial breaching. Here, four wave-dominated sandspits are compared to determine their common behavior. The study sites at river mouths have in common a high control of waves on longshore sediment transport leading to sandspit development; the Langue de Barbarie at the Senegal River delta, the Bouche du Roi at the mouth of the Mono River in Benin, the Mataquito River mouth in Chile, and the Pomene River mouth in Mozambique, each characterized by unique hydrodynamic conditions and geomorphologic features that influence their evolution and susceptibility to natural and anthropogenic impacts. Their cycles of opening and development, typically spanning decades, are studied by collecting 37 years of shoreline and wave reanalysis data from the Landsat and Sentinel-2 missions. It is shown that part of the morphodynamics is truly intrinsic and that climatic wave evolution drives only a small part of their evolution. A simplified model is introduced to predict the cyclic behavior of spits. The proposed model for sandspit development is based on a cyclic behavior, where newly formed spits mature and eventually break, resetting the cycle. This cyclic perception is represented as a function of time, where the elongation of the spit relative to its maximum length is modeled as a function of time and a constant wave-driven longshore sediment transport component. The model is tested at several sites with similar environmental conditions and blindly at one site with reasonable results. The present work also highlights the importance of spit evolution and the associated variability they impose on coastal downdrift and updrift, especially when considering anticipating the implementation of engineering solutions.

1. Introduction

Sandspits, on wave-exposed coastlines can be attractive areas for coastal communities. As they are located in tidal inlets or rivermouth outlet areas of mixing of fresh and salt water and of access to the sea/ocean, they are generally associated with rich natural habitats [Pradhan et al., 2015], and are favorable for human settlement, are commonly densely populated and their over-exploitation can lead to the fragility of ecosystems they host [Huamantinco Andrea Huamantinco Cisneros et al., 2016]. Sandspits also play an important role in backspit protection by acting as buffers against waves [Robin et al., 2020, Pellerin Le Bas et al., 2022]. Coastal zones around sandspits have a complex and dynamic morphological behavior [Duncan et al., 1984, Murray Hicks et al., 1999, Fenster and Dolan, 1996; Levoy et al., 2023]. The spit behavior itself is generally described by three main mechanisms; 1) Spit elongation by sediment accumulation at its tip introduced by longshore transport, 2) accretion at the end of a barrier spit bordering a tidal inlet – usually associated with erosion patterns on the opposite side of the inlet – and 3) the less common self-generating spit (a spit that does not require external sediment availability to elongate) [Aubrey and Gaines, 1982]. Wave-dominated inlets, where sandspit formation is most likely, are most often associated with the first mechanism. These spits are dominantly formed by wave-induced currents that transport sediments that are gradually deposited on an elongated feature [Aubrey and Gaines, 1982, Marcel et al., 2002]. A spit progressively elongates – toward the direction of Longshore Sediment Transport (LST) – as sand accumulates at its end, and its growth rate is directly related to the LST and the depth of water into which the spit grows [Dean and Dalrymple,

* Corresponding author.
E-mail addresses: adelaide.taveneau@gmail.com (A. Taveneau), rafael.almar@ird.fr (R. Almar), erwin.bergsma@cnes.fr (E.W.J. Bergsma).

https://doi.org/10.1016/j.ecss.2024.108798
Received 30 May 2023; Received in revised form 4 May 2024; Accepted 7 May 2024
Available online 21 May 2024

2001; Evans, 1942; Allard et al., 2008]. Its morphological changes depend on many parameters such as interactions between wave transformation [Ashton et al., 2016; Allard et al., 2008], tidal exchange [Powell et al., 2006; Robin et al., 2007], LST [Evans, 1942; Schwartz, 1982], river discharge [Chaumillon et al., 2014; Adams et al., 2016], sediment availability [Hequette and Ruz, 1991; Aubrey and Gaines, 1982], winds and tides [Pellerin Le Bas et al., 2022, Robin et al., 2020; Levoy et al., 2023], sea level rise [Hequette and Ruz, 1991], and human intervention [Allard et al., 2008; Lorenzo et al., 2007; Nahon et al., 2019]. Spit development is dependent on the interactions of the spit sand body with the hydrodynamics and sediment dynamics prevailing at river mouths, and in the case of tidal inlets, with ebb-tidal deltas. Several knowledge gaps have been identified in the literature on ebb-tidal deltas, for instance, including a poor understanding of their sediment dynamics, the influence of human interventions (such as dredging or coastal engineering) on their morphology and behavior, and their long-term response to sea-level rise and climate change, all of which can impact spit behavior. The opening and closing of inlets, and the associated significant morphological changes, can have economic and societal impacts by affecting, for instance, shipping channels, saltwater intrusion [Pradhan et al., 2015, Dada et al., 2021], or by increasing the risk of coastal flooding [Nguyen et al., 2020, Anthony, 2015]. These knowledge gaps highlight the need for further studies and research to improve our understanding of these complex coastal features. The geometry and evolution of the inlet, i.e. the length and width of the spit and the rate of elongation, are subject to influences at different timescales [Nicholas C Kraus, 1999]. The same knowledge gaps also apply to the interaction of river mouths with adjacent spits, especially during strong river flow [Anthony and Blivi, 1999, Cooper, 2001, Anthony, 2015, Zăinescu et al., 2021]. Tidal inlets, but also river mouths especially in semi-arid or arid areas or where flow can become extremely low seasonally, can be closed by large waves associated with strong longshore sediment transport [Merritt, 1974, Aouiche et al., 2023; Cienfuegos et al., 2017]. In these latter examples, sediment accumulation at the end of the spit can lead to such an extension that the tidal inlet or river outlet becomes situated several kilometers downdrift.

The flow of water either becomes inefficient, so that the water naturally finds another, easier route, or in some other cases a breach intervention may be necessary to protect coastal infrastructure or endangered ecosystems. Small natural breaches, a few to several meters wide, can easily become large inlets that either cause important economic and societal losses [Schmeltz et al., 1982, Ty and Kraus, 2005, Laïbi et al., 2014] or initiate erosion trends on the "up-drift" part of the spit [Iulian Zăinescu et al., 2019, Taveneau et al., 2021]. The Senegal river sandspit in Senegal is such an example: the inlet was so far down-drift from the river mouth that an artificial breach was urgently created to alleviate the water level in the "up-drift" city due to strong flooding episodes [Bergsma et al., 2020, Sadio et al., 2017, Anthony, 2015, Ndour et al., 2018]. This single breach, a few meters wide, became the new river mouth. The natural sandspit cycle was thus reset [Taveneau et al., 2021; Sadio et al., 2017], this most likely coincided with an "up-drift" erosion pattern on the ocean side of the city of St. Louis [Bergsma et al., 2020; Taveneau et al., 2021].

Breaching is in fact one of the mechanisms that drives spit migration and controls it with other parameters such as spit width [Pierce, 1969, Stephen, 1979, Zaremba and Leatherman, 1984; Boothroyd, 1985]. Natural breaches typically occur during natural sudden energetic events such as hurricanes, severe cyclones [Iulian Zăinescu et al., 2019, Villagran et al., 2011] and strong storm events [Schoonees et al., 1999, Iulian Zăinescu et al., 2019]: in which the narrower the sandspit, the more likely the breach [Masselink and van Heteren, 2014]. Several analytical models – for wave-dominated sandspits – have been implemented to predict their growth rate [Nicholas C Kraus, 1999, Palalane et al., 2014, Nguyen et al., 2020, Marcel et al., 2009] and with the growth length a linearly proportional inlet migration pattern [Nicholas C Kraus, 1999, Tran et al., 2009]. The spit width, on the other hand, is inversely proportional to the spit growth rate [Nicholas C Kraus, 1999, Nguyen et al., 2020]: when an inlet has largely migrated down-drift, the spit is more likely to naturally breach [Masselink and van Heteren, 2014].

Satellite Earth observation now provides unparalleled observation to study sandspits and large coastal features [Benveniste et al., Melet et al., 2020; Turner et al., 2021], especially in poorly documented regions [Almar et al., 2023]. Regular revisit open-source.

Landsat and Sentinel-2 data are particularly valuable in this area because they allow the collection of an image approximately every 8 days [Medina-Lopez, 2020]. This makes it possible to monitor the coastline on seasonal to interannual scales, the scales for coastal management. In this sense, effective assimilation of satellite data using machine learning is very promising. Satellite data are used to predict sandspit evolution [Taveneau et al., 2021] and eight different time series forecasting methods for predicting future shorelines on sandy coasts using historical satellite derived shorelines are compared [Calkoen et al., 2021]. Coastal studies are strengthened by examining the cross-sectional and local stability of inlets using the *InletTracker* tool as well as *CoastSat* [Vos et al., 2019], which is freely available online. This provides an unprecedented amount of information on inlet dynamics [Bergsma et al., 2020].

Here we compare four documented wave-dominated sandspits worldwide to determine their common behavior, focusing on spit elongation due to down-drift sediment accumulation. By collecting satellite and wave hindcast data over 37 years, we study the individual sandspit cycles of opening, development, migration, and behavior. This is done to determine whether sandspit dynamics are climatically or intrinsically forced, with the perspective of providing a conceptually simplified predictive tool for decision makers.

2. Methods and data

2.1. Satellite imagery and shoreline extraction

Here, shorelines are used as a proxy to evaluate the morphodynamics of our selected deltas and estuarine systems, in particular to track their spit/barrier evolution. For this purpose we use the open source Python toolkit *CoastSat* [Vos et al., 2019]. Within the *CoastSat* set of routines, publicly available optical satellite imagery can be downloaded, starting with Landsat 5 data acquired by NASA in 1984. Earlier versions of Landsat are not used due to inconsistencies in pixel resolution and coverage. Landsat 6 never reached orbit, but since 1999 the Landsat dataset includes Landsat 7 (1999), Landsat 8 (2013) and soon Landsat 9 (2021). The ground sampling distance, the pixel size, is constant over this period at a maximum of 30 m for the color bands and 15 m resolution for the panchromatic band. Note that the multispectral bands are pansharpened to 15 m within the *CoastSat* tool (although this has no resolution improvement on pixel ratios such as the NDWI). The revisit interval at the same location is typically every 16 days. In addition to Landsat data, Sentinel 2 data is also available. As part of the European Copernicus program, 2 satellites with optical sensors have been launched; S2A (2015) and S2B (2017) – S2C and D are planned for the coming years. Sentinel 2 A and B provide optical satellite imagery at 10 m resolution with a revisit interval depending on the latitude, but at worst every 5 days at the equator, enabling high-frequency coastal studies [Bergsma and Almar, 2020].

For Landsat and Sentinel satellite optical imagery, the *CoastSat* tool provides a trained machine learning model to classify sea, land, white water, and beach on a pixel-by-pixel basis. The pixel classification is used to optimize the use of the Modified Normalized Difference Water Index (MNDWI), excluding pixels related to white water and land, and focusing on the interface between water and sand pixels. An optimal shoreline position is then found using an Otsu procedure by minimizing the variance between the MNDW indices. The procedure is rather summarized here, for all details we refer to [Vos et al., 2019].

The *CoastSat* tool is globally applicable, but for each region of interest, study site, one sub-samples the satellite optical images. In this case, we only sample the satellite optical imagery around the sandspits up to their maximum observed length.

2.2. Study sites

River deltas, and the type of ebb/flood deltas, sandspit development, and barrier islands that go with them, are generally classified by the relative dominance of tidal vs. wave energy [Davies, 1980]. There are five classes; tidal dominated (high/low), mixed energy (tidal/wave dominated), and wave dominated. For our study, we are interested in ebb deltas that contain sandspits, and therefore focus on a relatively large importance of incident waves rather than tides. Here, we look for deltas with sandspits that are located in a similar environment: a wave-dominated micro-tidal environment with a strong oblique wave regime, which leads to a strong alongshore sediment transport and thus to a lengthening of the sandspit down-drift. However, to avoid concentration in a single area and still be globally representative, the four selected sites are distributed around the world (Fig. 1): *El Peñon* Mataquito river mouth in Chile, the *Langue de Barbarie* at the Senegal river delta in Senegal, the *Bouche du Roi* at the Mono river mouth in Benin, and the Pomene river mouth in Mozambique (Fig. 2).

The *El Peñon* delta is located in Chile (western South America, western central Chile; Fig. 1). Where the *Mataquito* River meets the Pacific Ocean (Fig. 2). With a mean wave height of $H_S = 2.7$ m and a peak period of $T_P = 11.7$ s [Villagran et al., 2011] and a semidiurnal tidal regime with a mean tidal range of 0.9 m, the *El Peñon* delta is strongly wave dominated. The delta is exposed to a predominantly southwesterly incident wave climate, resulting in the formation of sandspits associated with sediment accumulation [Cienfuegos et al., 2014] induced by wave-driven alongshore currents and sediment transport. The *El Peñon* delta was exposed to the 2010 Chilean tsunami, resulting in the complete disappearance of the sandspit. Interestingly, the initial recovery was rapid and a sandspit reformed over the following year [Villagran et al., 2011].

The *Langue de Barbarie* sandspit (West Africa, Northern Senegal; Fig. 1) is located at the city of Saint Louis, where the Senegal river enters the Atlantic Ocean (Fig. 2). The delta of the Senegal River is exposed to one of the most energetic, constant swells, considering a mean wave height of $H_S = 1.52$ m and a mean peak period of $T_P = 9.23$ s [Sadio et al., 2017]. The semi-diurnal tidal regime has a mean tidal range of 1.05 m. Thus, the combination of waves and tidal range makes the Senegal river estuary a strongly wave dominated estuary. It is interesting to note that the *Langue de Barbarie* is exposed to one of the strongest alongshore transport rates in the world, resulting in a strong down-drift, southward, migration of the inlet [Sadio et al., 2017; Almar et al., 2019; Taveneau et al., 2021]. This elongation of the sandspit (observed up to 40 km down-drift), would eventually lead to an inevitable natural breach of the barrier [FitzGerald et al., 2001], as the river tends to prefer the path of least resistance and generally results in flooding of the barrier/sandspit and thus a newly formed connection between the river and the ocean. In a natural system, this would not necessarily be a problem, but given the location of the city of Saint Louis, this process directly exposed the local population to the threat of flooding due to high water levels in the Senegal River. In October 2003, the water level in the Senegal River at the city was so high that flooding was imminent. In response, an artificial breach was created in the barrier island south of the city to relieve the population of the threat of flooding. The artificial breach rapidly widened within a few days and became the new mouth of the river. The *Langue de Barbarie* was, so to speak, re-initiated and, following the alongshore transport, migrated to the south. In doing so, and as a matter of disequilibrium, the stretching *Langue de Barbarie* was such that it led to significant up-drift erosion on the seaside of Saint Louis [Ndour et al., 2018; Bergsma et al., 2020; Taveneau et al., 2021].

The *Bouche du Roi* sandspit at estuary of the *Mono* river, is located in Benin (West Africa, Gulf of Guinea; Fig. 1) where the passage from Lake Aheme to the coast opens into the Atlantic Ocean (Fig. 2). The Mono Estuary is classified as a wave-dominated estuary considering a mean wave height varying between Hs = 0.5–1.5 m and a peak period between $T_P = 10$–15 s [Blivi et al., 2002] in combination with a semi-diurnal tidal regime with a mean tidal range of 1.05 m. This area is also exposed to strong oblique waves leading to an easterly alongshore drift (about 1×10^6 m^3/year) [Anthony and Blivi, 1999, Davies, 1980, Blivi et al., 2002, Abessolo et al., 2021, Korblah Lawson et al., 2021, Almar et al., 2015]. Until the construction of the deep-water harbors at Cotonou (1962) and Lomé (1967), the estuary seemed to experience an equilibrium between hydrodynamic forcing, geological configuration, and sediment supply and transport. After the introduction of the harbors, a significant unidirectional drift in the upstream direction was observed, leading to a large erosion of the downstream sandspit [Blivi et al., 2002]. In addition to the deep-water harbors that changed the geological configuration and sediment transport, the construction of the *Nangbéto* river dam – built between 1984 and 1987 – changed the sediment supply. In response, the

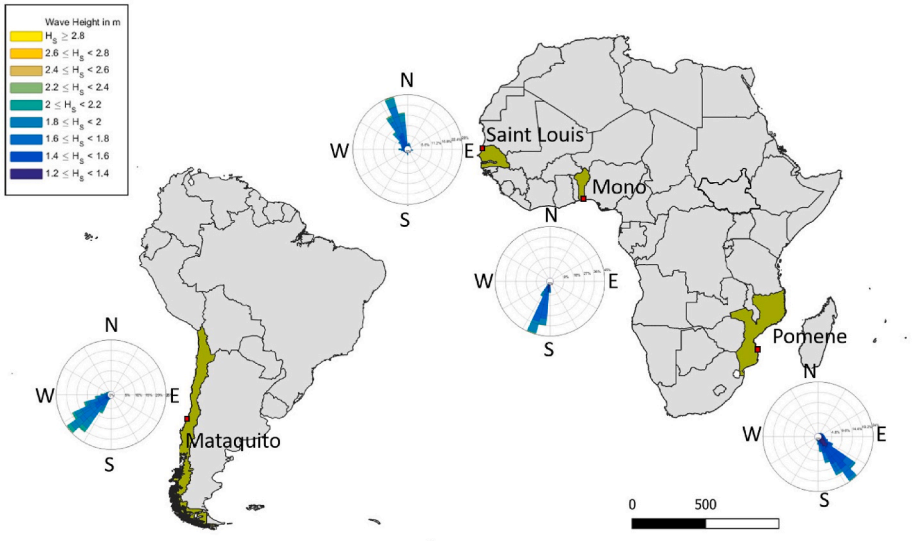

Fig. 1. Location of these study sites on the world map with their associated wave roses. The intensity on the wave roses represents the frequency of the significant wave height $_{HS}$ over the time period 1979–2016 (ERA5 data [Hersbach et al., 2018]).

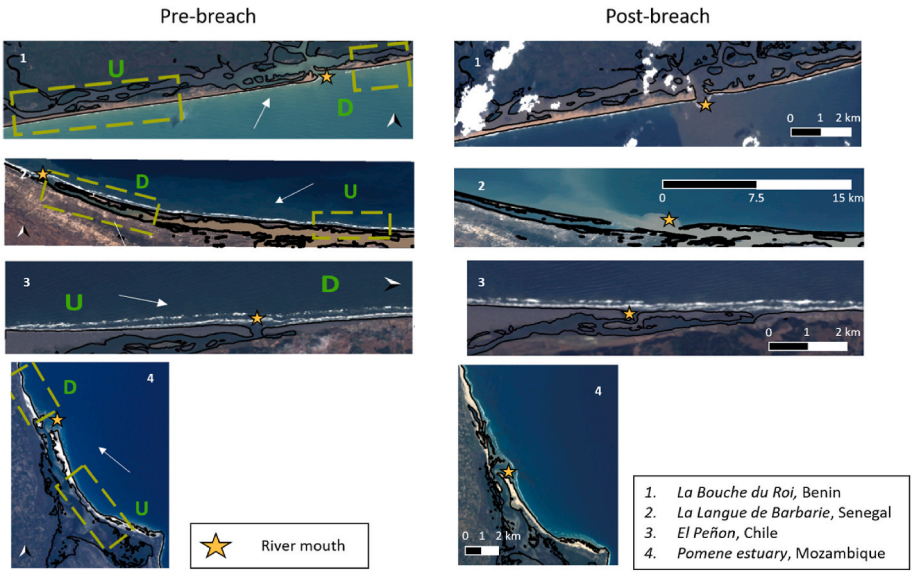

Fig. 2. Satellite images (Sentinel-2) of the sandspits before and after a breach: the *Langue de Barbarie* sandspit at the mouth of the Senegal river delta, the *Bouche du Roi* fronting the Mono river in Benin, *El Peñon* sandspit on Mataquito estuary in Chile, and the Pomene river sandspit in Mozambique. The white arrows represent the longshore sediment transport direction and the green squares on the are the delimitation of the *up-drift* (U) and *down-drift* (D) areas that are further studied. The river mouth is indicated with a yellow star for a better visibility. (For interpretation of the references to colour in this figure legend, the reader is referred to the Web version of this article.)

sandspit periodically reached its maximum length and closed the river mouth [Laïbi et al., 2012], thus reducing the cyclic life span. The *Mono* estuary closed in 1987, leading to a breach, either artificial or natural. Similar to the situation at Saint Louis in Senegal, two other artificial breaches were initiated in 1999 and 2009, respectively, to avoid flooding and erosion processes and to prevent the destruction of the village of *Djondji* [Laïbi et al., 2012]. The growth rate of this sandspit is about 700 m/year [Korblah Lawson et al., 2021].

The *Pomene* estuary (East Africa, Southern Mozambique; Fig. 1) is slightly different as it is more of a bay with a barrier island and, of the sandspit systems considered here, is the most exposed to tidal energy (Fig. 2). The *Pomene* estuary is in a mixed energy regime, wave/tide dominated, considering a mean wave height of H_S = 1.35 m, a peak period of T_P = 9.3 s (from [Hersbach et al., 2018] dataset) and the semi-diurnal tidal regime with a mean tidal range of 3 m. The bay faces the Indian Ocean, and the sandspit develops northwards in response to the prevailing southeasterly swell and associated alongshore sediment transport. The bay has been claimed to be threatened by coastal erosion due to climate change [Chemane et al., 1997]. The extension of the spit towards NNW is explained by sediment deposition associated with alongshore sediment transport [Massuanganhe and Arnberg, 2008]. The long-term erosion trend on the eastern side of the spit and its extension in the north-northwest direction have been observed by optical satellite imagery.

In addition to strong control by wave-driven longshore sediment transport, these sites share the fact that they are natural stretches of coastline that receive no artificial inputs that would influence results based on natural processes.

Wave reanalyses (Hs, Tp and Dir) are extracted from ERA5 (ECMWF) at the nearest node for each site. A basic form of annual longshore sediment transport is computed from these data by annually averaging the results of Kaczmarek et al., 2005], Kamphuis [Kamphuis, 1991], and Bayram's formula [Bayram et al., 2007]. While these coarse estimates provide a rough assessment, previous studies have shown that this first-pass estimate offer the right order of magnitude (see for *Saint Louis* and *Grand Popo* validation and limitation of the approach [Sadio et al., 2017; Almar et al., 2015, 2019; Taveneau et al., 2021]).

2.3. Conceptual model for the intrinsic dynamics of sandspits

As pointed out by e.g. [George, 1977, FitzGerald et al., 2001], sandspits follow a cyclic pattern in which newly formed sandspits mature, and when they reach their "old age" breakage occurs, eventually resetting the cycle. This cyclic perception of sandspit development and extension can be conceptually represented as a function of time as shown in [Taveneau et al., 2021]. According to this conceptual model, a cycle runs from $0 < \frac{x}{L} < 1$, and $x/L \rightarrow 1$ represents the moment when the elongation of the sandspit reaches its maximum, leading to a closure of the river mouth and/or a new breach. x is defined as the length of the spit, with the reference $x = 0$ being the maximum retraction of the spit. A breach is defined as a sudden change in x by visual inspection. Similar to the previous, the characteristic time scale is defined as the observed duration of the breaching-retreat-breaching cycles by fitting a model to the data.

Here, we propose a cyclic model based on a constant wave-driven alongshore sediment transport component $_Q$ (climatology mean) according to equation (1).

$$\frac{x}{L} = aQ\left(\frac{t}{T}\right)^b \tag{1}$$

where x = the length of the sandspit.

L = the maximum length of the sandspit
t = time
T = the period of a spit cycle
Q = longshore sediment transport [$m^3/year$]
a,b = scalar coefficients

For each sandspit, the length and time characteristics were normalized to the system length and period characteristics.

2.4. Spectral analysis of the coastline

Cyclical behavior can generally be analyzed well using Fourier analysis. However, it requires long time series. Here, according to the authors, the temporal variation of the cycle duration of the spits is be-

tween 10 and 42 years, but the time span of the satellite data is only 37 years. Here we address this problem by using a modified Discrete Fourier Transform (DFT), where the signal is extracted by convolution with cosines of given periods (from 1 to 40 years), which allows to resolve signals up to twice the observation period, but with lower temporal resolution.

$$PDST(T) = \sum_{T=1}^{T=40} var\left(signal(t) * cos\left(\frac{2\pi}{T}\right)\right) \quad (2)$$

where *PDS* is the power density spectrum, *signal* is the input signal - in this case the cross-shore position in time for a given point along the shoreline, $_T$ is the signal period in time, $T = 1$ year and $T = 40$ years are the minimum and maximum periods tested. For this analysis, one must ensure that the input signal is equidistantly sampled. This is often not the case for satellite derived products: depending on the location, the revisit interval varies due to satellite orbits, but also due to visibility (i.e. clouds) [Bergsma and Almar, 2020]. Therefore, the data have been resampled annually to ensure continuous data.

3. Results

3.1. Intrinsic versus forced dynamics

The conceptual sandspit model, as presented in section 3.3, allows us to identify the relative contribution of intrinsic cyclic behavior (effectively deactivating the temporal variability of $_Q$) and forced sandspit behavior by wave dynamics. In order to apply the conceptual spit model to the four selected sites, a measured spit length and cyclic period are required. For each of the sites, these two characteristics are derived from satellite optical imagery collected since 1984 by manually tracing the spit tip over time. This resulted in the following characteristics.

During the period analyzed, at least 2 (partial) cycles are observed per site: 2 cycles for Senegal river, 2 cycles for Mataquito, 3 cycles for Pomene, and 4 cycles for Mono, as indicated by the squares, diamonds, asterisks, and circles in Fig. 3, respectively. Together with the basic parameters (Table 1), we can now fit the observations to the conceptual model represented by equation (1). One might expect the exponential component in equation (1), *b*, to be greater than 1, allowing for increased migration rates as the tip moves away from its origin, as observed early in [Taveneau et al., 2021]. However, when fitted to the

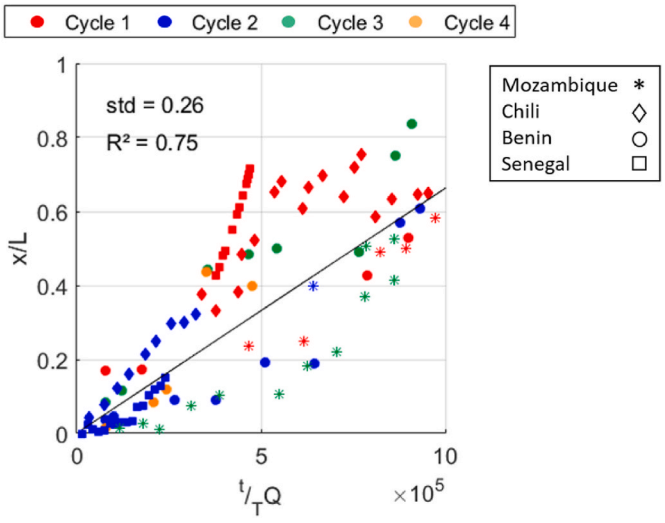

Fig. 3. Evolution of the sandspits length as a function of time per study sites (markers) derived from the CoastSat tool [Vos et al., 2019] with their associated cycles (colours), and fitted equation expressed as equation (1) (black line). (For interpretation of the references to colour in this figure legend, the reader is referred to the Web version of this article.)

Table 1
Sandspits characteristics: the maximum sandspit extension length (measured with observations) and the duration of a cycle of elongation/breaching (estimated with the conceptual model).

Sandspits	Length [km]	Period [years]
Mataquito river (Chile)	7.4	42
Mono river (Benin)	11.3	10
Senegal river (Senegal)	32	35
Pomene river (Mozambique)	12.9	24

observations, the coefficient b tends to 1, as indicated by the black line (Fig. 3). A $R^2 = 0.75$ for the different sites combined shows that the conceptual model performs quite well. In particular, the conceptual formulation depends on an average longshore sediment transport and should be considered as representative for the intrinsic spit development part over the study period from 1984 to 2021. It also means that external forcing such as climate regimes, irregular sediment supply (from varying river discharge or directional variations that alter the longshore sediment transport), sea level rise, are not considered in this conceptual model.

Forced behavior is seen here as sandspit behavior driven by temporally varying wave conditions. We can account for this by (re-)activating the temporal variability of Q in equation (1). Measured wave conditions, e.g. from wave buoys, do not exist in most of the selected areas, and therefore we use aggregated ERA-5 wave condition products distributed through the Copernicus Climate Data Store as part of the Copernicus Climate Change Service (C3S) [Hersbach et al., 2018]. By including time-varying wave conditions, we add a contributing component and expect to explain more of the observed variability. Fig. 4 a shows the time series of spit length (from top to bottom) at *Mataquito*, *Mono*, *Pomene* and *Saint Louis*. The vertical lines in the individual subplots per location denote cycle resets (a break or an event such as at *Mataquito*). From Fig. 4a it is clear that the conceptual spit model, which captures only the cyclic behavior, is largely in phase with the observations. However, the amplitude - the actual length of the sandspit - is more accurately captured when the cyclic and forced components are combined (yellow). This can be explained by the fact that the cyclic model is linear ($b \approx 1$) with no time-varying component. The estimation of the spit length diverges when the position of the spit tip oscillates (obvious for *Mataquito* and *Saint Louis*) due to the variability of the wave conditions. Consequently, adding the wave forcing improves the estimation of the spit length, as indicated by the improvement of the RMS error in Table 2. For the Mono sandspit in particular, we note that the inclusion of wave variability also reduces the phase shift between observations and model, as indicated by the high R^2 coefficient in Table 2.

Similarly, the two applications of the conceptual sandspit model, cyclic and cyclic + forced, allow an analysis of the relative contribution in terms of explained variance, as shown in Fig. 4 c and Table 2. At all different sites, the vast majority of the variance is explained by the intrinsic cyclic sandspit behavior. The average gain in explained variance is 4% when wave conditions are included. This tells us that resetting or breaching is predominantly a matter of time. However, where the spit tip is located, the actual position in time, is only weakly dependent on the wave variability to which it is exposed.

3.2. Vicinity imprints of sandspit signature

Now that we have developed a simple cyclic model for the spit tip in time, we investigate here how this dynamic affects its surroundings. To do this, a spectral analysis (3.4) is applied to time series along the coast, *up-drift*, *sandspit* where the entrance to the open ocean is from 0 to $x/L \rightarrow 1$ and the third zone is *down-drift*. For the sandspits of the *Mono*, Pomene and Senegal rivers, time series are shown along with their spatial boundaries in Fig. 5. The *Mataquito* river sandspit, is excluded from this analysis because the cyclic period is longer than the available shoreline

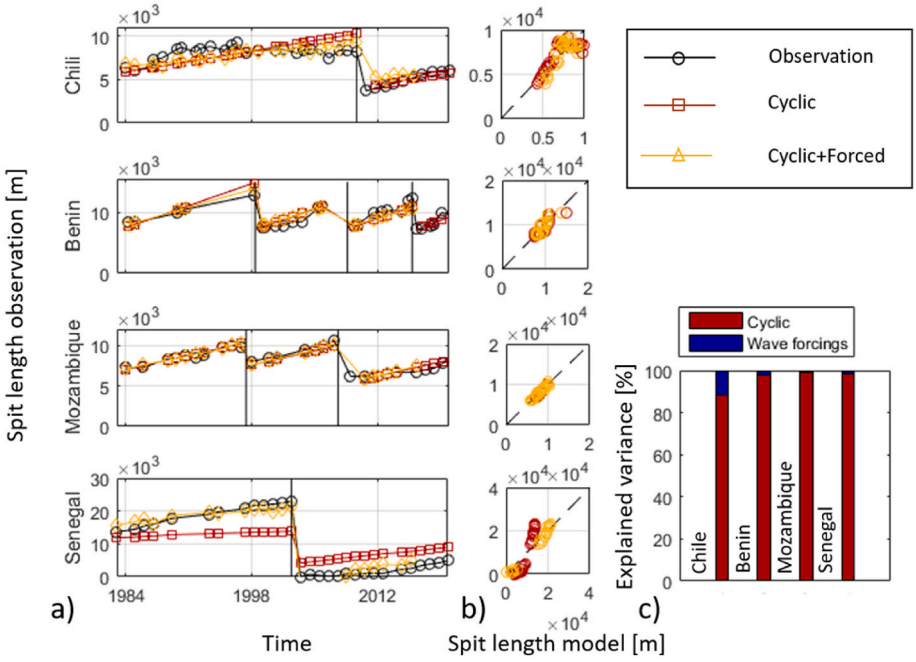

Fig. 4. (a) Evolution of sandspit length as a function of time between 1984 and 2021 – satellite data (black), projected data with the conceptual model (red), projected data with both the cyclic hypothesis and wave forcing (yellow) – for the four study sites with location of breaches (horizontal lines). (b) Linear regressions of sandspit length between observed data with model predictions and model predictions with wave forcing. (c) The explained variance with the observed data for the cyclic evolution of spit length (red), the evolution of spit length due to wave forcing only (blue). (For interpretation of the references to colour in this figure legend, the reader is referred to the Web version of this article.)

Table 2
Correlation coefficients per study site between the observed data and the conceptual model estimated ones with and without the wave forcings along with the associated RMS errors.

Sandspits	R2 Cyclic	R2 Cyclic + Forced	RMSE Cyclic	RMSE Cyclic + Forced
Mataquito river (Chile)	0.67	0.70	1.03 km	0.82 km
Mono river (Benin)	0.75	0.82	0.83 km	0.68 km
Pomene river (Mozambique)	0.93	0.95	0.34 km	0.33 km
Senegal river (Senegal)	0.94	0.97	5.66 km	1.56 km

time series. Since the present study focuses on inter-annual to decadal evolution, the cross-shore positions are aggregated annually and linearly interpolated for missing years at the beginning of the sampling period (early LandSAT imagery). This ensures a consistent data set, even with temporally sparse clear-sky imagery during rainy periods. The examined time series are shown in Fig. 5 (middle panel) per site, together with the annually averaged wave time series (top panel). In this data set and for the three study sites, sudden changes in time on the longshore axis (red), immediately followed by locally important cross-shore variations in the down-drift area (blue dashed line), are due to a breach occurring in the same down-drift area. These down-drift cross-shore variations physically correspond to the collapse or retreat of the down-drift sandspit caused by the breaching mechanism, this phenomenon being particularly visible for the Senegal and Mono sandspits. On the other hand, the up-drift time series (blue continuous line) are quite stable in time, and thus their cross-shore variation in time is less affected by the breaches occurring in the spit.

With respect to dominant time scales, in Fig. 5 the spectra in the bottom panels are computed from the time series shown in the middle panels. An energy peak in the spectra indicates a certain dominance of those frequencies in the time series. In the case of the *Mono* spit, the observed spit tip cycle period corresponds well to an energy peak in the up- and downdrift shoreline spectra, although the energy peak is more pronounced in the downdrift. For *Saint Louis*, the up- and down-drift shoreline spectra present a significantly shorter time scale than the found spit tip cycle period, more or less a third compared to the spit itself. For *Pomene*, the spectral analysis suggests a cyclic period in the order of 15 years and seems to be more driven by wave variability.

Of the three sites, the Mono sandspit has the shortest cycle and thus the largest number of cycles occurring during the study period. Therefore, special attention is given to the Mono sandspit in the analysis to determine the influence of the cyclical sandspit mechanism on the surrounding coastal stretches. Fig. 6, shows that there is a weak correlation between the cyclicity of the spit and the up-drift, while both the spit area and the down-drift have a clear influence on the cyclicity of the shoreline. Waves drive the cross-shore variability of the shoreline on the whole spit at high (8 years) and low frequency (23 years), but the elongation of the spit seems to be mostly driven by high-frequency phenomena, and mostly by its cyclicity (darker red area around the *Tcycle*).

4. Discussion

4.1. Sandspits as a major source of coastal variability

The results highlight a better agreement between the lengthening of the spits with the cyclic model than with the climate variability of the waves: the explained variance (Fig. 4c) shows that, on average over the four spits, 83% of the spit lengthening process is due to its natural cyclicity. In contrast, Fig. 5) shows that waves definitely have an impact when comparing wave variability with cross-shore shoreline evolution. This observation raises an important question: are cross-shore and longshore variations on wave dominated spits driven by different forcings? The case of the Mono sandspit is an illustration of this: in the longshore direction, one can see the distribution of factors that influence the cross-shore variation of the shoreline. The *up-drift* is in no way

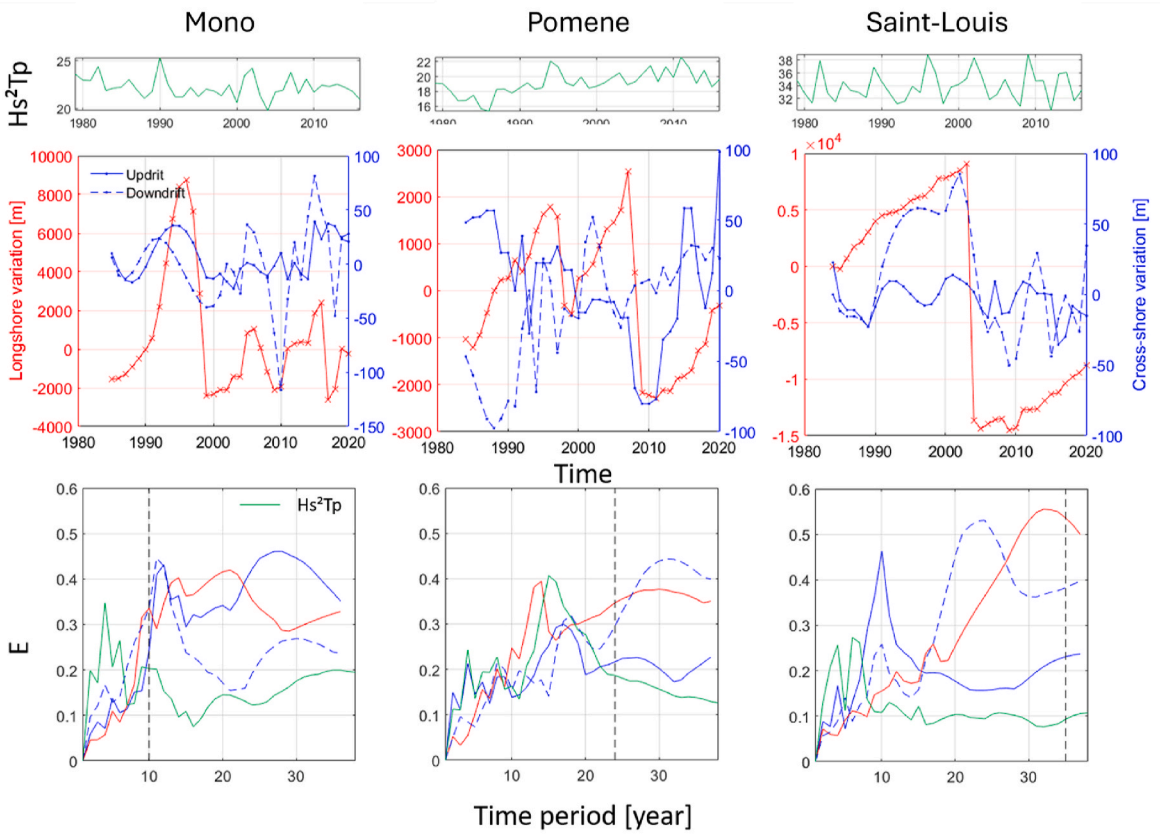

Fig. 5. (Top) Wave time series (1979–2016) annually averaged per site. (Middle) Spectral analysis of the cross-shore coastline variation up-drift and down-drift, and alongshore variation on the sandspit over the years for the four study sites. The vertical red dashed-line represents the cycle duration estimated with the conceptual model. The vertical dashed black line in Fig. 5 corresponds to the sandspit cycle period (*Tcycle*) as found in section 4.1 (i.e. maximum of sandspit alongshore position variance). (Bottom) Studied time series per zones: averaged cross-shore evolution of the up-drift and down-drift areas in blue and longshore evolution of the spits length in red. For better visibility, the median of each signal is subtracted. (For interpretation of the references to colour in this figure legend, the reader is referred to the Web version of this article.)

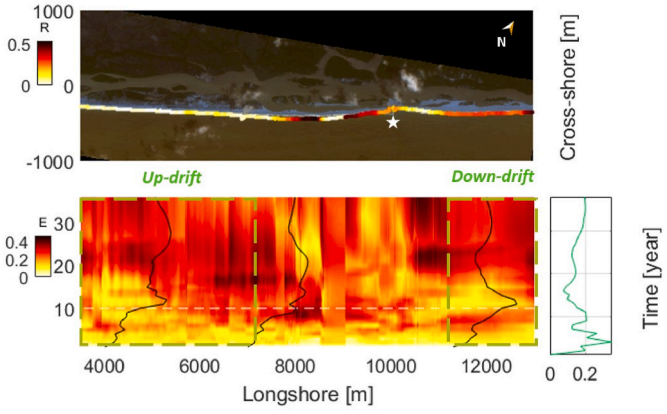

Fig. 6. Mono sandspit (Grand Popo, Benin): (Top) Correlation between the model output and the cross-shore variation over time map-projected onto a Sentinel-2 image. The white star indicates the position of the breach on the satellite image. (Bottom) Energy distribution over the shoreline cross-shore positions in time – the white horizontal dashed-line corresponds to the spit cycle, the black lines represent the zone-by-zone DFT. The wave parameters spectrum over time ($\frac{2}{Hs}$) is presented on the right in green as a point of comparison. To avoid the pixel to pixel noise, the time-series are averaged every 100 m. The cycle period is shown as a white dashed line for a better visualization. The found correlation maxima are also visible as energy maxima (red shades) at the *Tcycle* position. (For interpretation of the references to colour in this figure legend, the reader is referred to the Web version of this article.)

influenced by the cyclical development of the spit, only by high and low frequency wave forcing (an residual). But the tip of the spit – where the breaches occurred – and thus its length, is influenced by waves and its intrinsic evolution with cyclicity as its predominant driver. Finally, the down-drift area is modulated by both drivers. It should be noted that the observed down-drift timescales also have higher frequencies than the spit itself. This has been observed elsewhere and can be attributed to sand transported by longshore current entering the inlet through sandbars that break away from the up-drift side, migrate across the mouth and weld to the down-drift side [Burvingt et al., 2022, Nicholas C Kraus, 1999, Nicholas and Galgano, 2001, Robin et al., 2020, Pellerin Le Bas et al., 2022].

Sandspit elongation models through the literature are mainly based on the longshore sediment transport variability as the most influential factor for spit elongation [Nicholas C Kraus, 1999, Palalane et al., 2014, Nguyen et al., 2020, Minh Duong et al., 2017, Ranasinghe et al., 1999, Marcel et al., 2009] and suggest that the elongation is directly proportional to the longshore sediment transport rate and depends on fundamental geometric parameters and time. In this study we can also emphasize, through the investigation of the *Bouche du Roi* spit (section 4.2), that longshore sediment transport variability has only a limited effect on the morphology of a spit. However, our results indicate that the overall behavior of a sandspit is under the combined influence of climate and cyclic forcing.

4.2. A prediction tool for coastal management around sandspits

Sandspits play an important role in coastal ecosystem diversity,

commonly act as efficient wave-buffers by protecting back-spit populations and infrastructure, attract human settlements, and many are important economically, including for tourism. As a spit's length has a major impact on the economic and ecosystem services it provides, a prediction tool for spit extension is key for decision-making in order to preserve local populations and their activities, and ecosystems and services. Breaches – referred to as the beginning of a spit cycle in this study – are responsible for extreme shoreline retreat of the up-drift area [Iulian Zăinescu et al., 2019] on the cross-shore axis, endangering communities and compromising infrastructures. Knowledge of the following wave-dominated spit parameters: longshore sediment transport, maximum length of the spit, and its growth rate, allows the possibility of a rough prediction of the date of mouth closure [Tran et al., 2012]. This estimate could be used to anticipate the decision to open artificial breaches to avoid a disaster like that of Saint Louis city (Senegal) in 2003 [Sadio et al., 2017; Bergsma et al., 2020] (described in section 3.2).

To strengthen our conclusions on the applicability of our cyclic model, a blind application of our model on a well-documented sandspit is proposed here to discuss its relevance. The Cap Ferret is a very dynamic and wave-dominated sandspit [Marcel et al., 2002, Nahon et al., 2019]. To test our cyclical conceptual model for sandspits, this section applies equation (1) to the Cap Ferret to see if the observed *Tcycle* can be predicted from the spit parameters given in Table 3.

During the last decades this spit has been migrating southward – which is also the longshore sediment transport direction – and sometimes reached the southern edge of the inlet and merged with it. The autocycle hypothesis of this landform was raised and estimated with a period of about 80 years [Michel and Howa, 1997]. Two *Tcycle* were calculated based on the minimum and maximum values of spit growth, and the average of these two values is taken as the final estimate of *Tcycle* with our conceptual model. Here we find $Tcycle \simeq 84$ years. The literature, which our prediction is based on the conceptual model, shows great agreement here. While our model still needs to be confronted with other sandspits in different environments, our hypothesis of the cyclic nature of sandspits seems to be valid and should be further investigated.

4.3. Inherent limitations of the data

The satellite imagery used in this study provides a regional spatial understanding; the pixel resolution varies between 10 m and 30 m, depending on the satellite mission from which the data originate. The derived shorelines are accurate to within a ± 10 m (or ± 30 m) error. We consider this error to be as the sandspit scale is kilo-metric.

The quality of our model regression with the data and spectral analysis is affected by the lack of data over time. Changes in spit morphology that occur on a regional scale are extremely long processes – several decades – as shown in this study. Since the open access satellite data start in 1984, one can only study the morphodynamics of sandspits over a period of 38 years, when there are not too many gaps in the data. Considering the estimated cycle duration – which varies between 10 and 42 years in our study – the lack of data on a temporal scale has a particular impact on the frequency analysis (section 3.4). Our conceptual model relies only on the hypothesis that spit elongation is climate-free; the elongation process does not depend on longshore sediment transport variability in time.

For example, in section 3.4, one may wonder why the cycle period peak is not the one that prevails for the Senegal sandpit, as it seems to match in the case of *Mono* and *Pomene* sandspits. This spit cycle duration is about 35 years, while we have access to 37 years of data (if there is no gap in the data) with the open access satellite imagery.

Table 3
The cap Ferret sandspit characteristics based on literature [Marcel et al., 2002, Nahon et al., 2019].

Length	28 km
Qmean	0.63×10^6 $m^3/year$
Growth rate	100–250 $m/year$

4.4. Cyclic model parameters

The chosen model type (equation (1); section 3.3) can also be discussed. Physically speaking, $b = 1$ means that the same amount of sand is captured by the spit every year. Since our model is based on the hypothesis that spit elongation depends on the longshore sediment transport temporally averaged value, $b = 1$ implies that the sediment bypass varies with the longshore sediment transport: if the longshore sediment transport increases, the sediment bypass increases and vice versa. $b < 1$ would mean that the farther the tip of the spit is from the mouth of the river, the slower its migration rate. Assuming that $t \to \infty$, the length of the spit will tend to stabilize around a certain value. Looking back at Fig. 3, it seems that this was the case for the *El Peñon* spit in Chile (red diamonds) before the tsunami destroyed the spit in 2010, initiating the beginning of a new cycle. In contrast, $b > 1$ would imply that the further away the spit is from the mouth of the river, the higher its migration rate. In the study [Taveneau et al., 2021], the same methodology was applied to the Senegal river sandspit alone, with the difference that the parameter *b* depends on the longshore sediment transport. It was found that the farther the tip of the spit is from the mouth of the river, the greater the migration rate. In this study, the total power coefficient was greater than 1 and can be discussed here. Since the width of the spit is inversely proportional to its length [Nicholas C Kraus, 1999, Nguyen et al., 2020], some of the sediment material that comes from the eroding upstream part and the sediment bypass partly accumulates at the tip of the spit [Aubrey and Gaines, 1982]. For the case of the Senegal sandspit, it has been estimated that the sandspit can capture up to 35% of this sand volume [Taveneau et al., 2021].

One could ask if there is a stable position of the spit, where the tip of the spit would be far enough away from the up-drift part so that there is no negative feedback on the beach width (erosion pattern), and at the same time close enough not to block commercial activities (fishing) with a river mouth too far away from inhabited areas (see Senegal for example). Such a position could be evaluated, assessing the pros and cons of both the economic impact and the local impact on beach width.

5. Conclusion

In this study, a cyclic climate-free conceptual model is proposed for the wave-driven lengthening process of sandspits. Satellite imagery over a long acquisition period (37 years) allowed the monitoring of sandspit evolution at a regional scale. Shorelines were derived from four sandspits (Senegal river mouth in Senegal, Mono in Benin, Pomene in Mozambique, and Mataquito in Chile) that share similar environmental conditions with oblique waves, large LST and micro-tidal conditions. The overall results show that 83% of a wave-dominated spit elongation process is self-evolving, cyclical, and affects shoreline downdrift. Our model was applied to a spit that was not part of the sample used to build it, Cap Ferret at the inlet of the Arcachon lagoon (France), to assess its reliability. The key cycle period was correctly captured, which gives confidence in our predominant cyclical observation of sandspits and our proposed model. However, the morphology of sandspits depends on many influences, not all of which have been taken into account here, in particular the primary influence of human activity. Nevertheless, such a physically reduced predictive model can be easily implemented at other wave-dominated sandspits to support coastal protection strategies (artificial breaching, down drift beach management).

CRediT authorship contribution statement

Adélaïde Taveneau: Writing – original draft, Validation, Methodology, Investigation, Formal analysis, Data curation. **Rafael Almar:**

Writing – original draft, Supervision, Methodology, Validation. **Erwin W.J. Bergsma:** Supervision, Writing – review & editing.

Declaration of competing interest

The authors declare that they have no known competing financial interests or personal relationships that could have appeared to influence the work reported in this paper.

Data availability

Data will be made available on request.

References

Abessolo, Grégoire O., Larson, Magnus, Almar, Rafael, et al., 2021. Modeling the bight of Benin (gulf of Guinea, west africa) coastline response to natural and anthropogenic forcing. Regional Stud. Mar. Sci. 48, 101995.

Adams, Peter N., Keough, Katherine Malone, Olabarrieta, Maitane, 2016. Beach morphodynamics influenced by an ebb-tidal delta on the north Florida atlantic coast. Earth Surf. Process. Landforms 41 (7), 936–950.

Allard, J., Bertin, X., Chaumillon, E., Pouget, F., 2008. Sand spit rhythmic development: a potential record of wave climate variations? arçay spit, western coast of France. Mar. Geol. 253 (3), 107–131. https://doi.org/10.1016/j.margeo.2008.05.009. ISSN 0025-3227.

Almar, Rafaël, Kestenare, Elodie, Reyns, J., Jouanno, Julien, Anthony, E.J., Laibi, R., Hemer, Mark, Du Penhoat, Y., Ranasinghe, Roshanka, 2015. Response of the bight of Benin (gulf of Guinea, west africa) coastline to anthropogenic and natural forcing, part1: wave climate variability and impacts on the longshore sediment transport. Continent. Shelf Res. 110, 48–59.

Almar, R., Kestenare, E., Boucharel, J., 2019. On the key influence of remote climate variability from tropical cyclones, north and south atlantic mid-latitude storms on the senegalese coast (west africa). Environ. Res. Commun. 1 (7).

Almar, Rafael, Stieglitz, Thomas, Addo, Kwasi Appeaning, Ba, Kader, Ondoa, Gregoire Abessolo, Bergsma, Erwin WJ., Bonou, Frédéric, Dada, Olusegun, Angnuureng, Donatus, Arino, Olivier, 2023. Coastal zone changes in west africa: challenges and opportunities for satellite earth observations. Surv. Geophys. 44 (1), 249–275.

Andrea Huamantinco Cisneros, M., Revollo Sarmiento, Natalia V., Delrieux, Claudio A., Cintia Piccolo, M., Perillo, Gerardo M.E., 2016. Beach carrying capacity assessment through image processing tools for coastal management. Ocean Coast Manag. 130, 138–147. https://doi.org/10.1016/j.ocecoaman.2016.06.010. ISSN 0964-5691. https://www.sciencedirect.com/science/article/pii/S0964569116301193.

Anthony, E.J., 2015. Patterns of sand spit development and their management implications on deltaic, drift-aligned coasts: the cases of the Senegal and volta river delta spits, west africa. In: Randazzo, G., Jackson, D., Cooper, J. (Eds.), Sand and Gravel Spits. Coastal Research Library, Cham. Springer, pp. 21–36.

Anthony, E.J., Blivi, A.B., 1999. Morphosedimentary evolution of a delta-sourced, drift-aligned sandbarrier–lagoon complex, western bight of Benin. Mar. Geol. 158, 161–176. https://doi.org/10.1016/S0025-3227(98)00170-4.

Aouiche, Ismail, Sedrati, Mouncef, Anthony, Edward J., 2023. Modelling of sediment transport and deposition in generating river-mouth closure: oum-errabia river, Morocco. J. Mar. Sci. Eng. 11 (11), 2051.

Ashton, A.D., Nienhuis, J., Ells, K., 2016. On a neck, on a spit: controls on the shape of free spits. Earth Surf. Dyn. 4 (1), 193–210.

Aubrey, D.G., Gaines, A.G., 1982. Rapid formation and degradation of barrier spits in areas with low rates of littoral drift. Mar. Geol. 49 (3), 257–277. https://doi.org/10.1016/0025-3227(82)90043-3. ISSN 0025-3227. https://www.sciencedirect.com/science/article/pii/0025322782900433.

Bayram, Atilla, Larson, Magnus, Hanson, Hans, 2007. A new formula for the total longshore sediment transport rate. Coast. Eng. 54 (9), 700–710.

Jérôme Benveniste, Anny Cazenave, Stefano Vignudelli, Luciana Fenoglio-Marc, Rashmi Shah, Rafael Almar, Ole Andersen, Florence.

Bergsma, Erwin W.J., Almar, Rafael, 2020. Coastal coverage of esa' sentinel 2 mission. Adv. Space Res. 65 (11), 2636–2644. https://doi.org/10.1016/j.asr.2020.03.001. ISSN 0273-1177.

Bergsma, E.W.J., Sadio, M., Sakho, I., Almar, R., Garlan, T., Gosselin, M., Gauduin, H., 2020. Sand-spit evolution and inlet dynamics derived from space-borne optical imagery: is the Senegal-river inlet closing? J. Coast Res. (Special Issue No. 95), 372–376. ISSN 0749-0208.

Blivi, Adote, Anthony, Edward J., Oyédé, Lucien M., 2002. Sand barrier development in the bight ofbenin, west africa. Ocean Coast Manag. 45, 185–200.

Boothroyd, Jon C., 1985. Tidal inlets and tidal deltas. In: Coastal Sedimentary Environments. Springer, pp. 445–532.

Burvingt, Olivier, Nicolae Lerma, Alexandre, Bertrand, Lubac, Mallet, Cyril, Senechal, Nadia, 2022. Geomorphological control of sandy beaches by a mixed-energy tidal inlet. Mar. Geol. 450, 106863.

Calkoen, Floris, Luijendijk, Arjen, Rivero, Cristian Rodriguez, Kras, Etienne, Baart, Fedor, 2021. Traditional vs. machine-learning methods for forecasting sandy shoreline evolution using historic satellite-derived shorelines. Rem. Sens. 13 (5), 934.

Chaumillon, Eric, Ozenne, F., Bertin, X., Long, Nathalie, Ganthy, F., 2014. Wave climate and inlet channel meander bend control spit breaching and migration of a new inlet: La coubre sandspit. J. Coast Res. 70, 109–114.

Chemane, David, Motta, Helena, Achimo, Mussa, 1997. Vulnerability of coastal resources to climate changes in Mozambique: a call for integrated coastal zone management. Ocean Coast Manag. 37 (1), 63–83.

Cienfuegos, Rodrigo, Villagran, Mauricio, Aguilera, Juan Carlos, Catalán, Patricio, Castelle, Bruno, Almar, Rafael, 2014. Video monitoring and field measurements of a rapidly evolving coastal system: the river mouth and sand spit of the mataquito river in Chile. J. Coast Res. 70, 639–644.

Cienfuegos, Rodrigo, Rafael Campino, José, Gironás, Jorge, Almar, Rafael, Villagrán, Mauricio, 2017. River Mouths and Coastal Lagoons in Central chile. The Ecology and Natural History of Chilean Saltmarshes, pp. 15–46.

Cooper, J.A.G., 2001. Geomorphological variability among microtidal estuaries from the wave-dominated south african coast. Geomorphology 40 (1–2), 99–122.

Dada, Olusegun, Almar, Rafael, Morand, Pierre, Ménard, Frédéric, 2021. Towards west african coastal social-ecosystems sustainability: interdisciplinary approaches. Ocean Coast Manag. 211, 105746.

Davies, J.L., 1980. Geographical Variation in Coastal Development, second ed. Longman, London, p. 212.

Dean, R.G., Dalrymple, R.A., 2001. Long-term processes. In: 2001 Cambridge: Cambridge University Press. Coastal Processes with Engineering Applications, pp. 35–70.

Duncan, M Fitzgerald, Shea, Penland, Nummedal, D.A.G., 1984. Control of barrier island shape by inlet sediment bypassing: east Frisian islands, west Germany. Mar. Geol. 60 (1–4), 355–376.

Evans, O.F., 1942. The origin of spits, bars, and related structures. J. Geol. 50 (7) https://doi.org/10.1086/625087.

Fenster, Michael, Dolan, Robert, 1996. Assessing the impact of tidal inlets on adjacent barrier island shorelines. J. Coast Res. 294–310.

FitzGerald, Duncan M., Buynevich, Ilya V., Rosen, Peter S., 2001. Geological evidence of former tidal inlets along a retrograding barrier: duxbury beach, Massachusetts, USA. J. Coast Res. 437–448.

George, F Oertel, 1977. Geomorphic cycles in ebb deltas and related patterns of shore erosion and accretion. J. Sediment. Res. 47 (3), 1121–1131.

Hequette, Arnaud, Ruz, Marie-Helene, 1991. Spit and barrier island migration in the southeastern canadian beaufort sea. J. Coast Res. 677–698.

Hersbach, H., Bell, B., Berrisford, P., Biavati, G., Horányi, A., Muñoz Sabater, J., Nicolas, J., Peubey, C., Radu, R., Rozum, I., Schepers, D., Simmons, A., Soci, C., Dee, D., Thépaut, J.-N., 2018. Era5 hourly data on single levels from 1979 to present. Copernicus Clim. 10, 10.24381. Change service (c3s) climate data store (cds).

Iulian Zăinescu, Florin, Vespremeanu-Stroe, Alfred, Tătui, Florin, 2019. The formation and closure of the big breach of sacalin spit associated with extreme shoreline retreat and shoreface erosion. Earth Surf. Process. Landforms 44 (11), 2268–2284.

Kaczmarek, Leszek M., Ostrowski, Rafal, Pruszak, Zbigniew, Rozynski, Grzegorz, 2005. Selected problems of sediment transport and morphodynamics of a multi-bar nearshore zone. Estuarine. Coast. Shelf Sci. 62 (3), 415–425.

Kamphuis, J William, 1991. Alongshore sediment transport rate. J. Waterw. Port, Coast. Ocean Eng. 117 (6), 624–640.

Korblah Lawson, Stephan, Tanaka, Hitoshi, Udo, Keiko, Hiep, Nguyen Trong, Xuan Tinh, Nguyen, 2021. Evaluation of sandspit growth and longshore sediment transport rates at the "bouche du roi" inlet, benin, using remotely sensed images. J. Japan Soc. Civil Eng., Ser. B1 (Hydraulic Eng.) 77 (2), I_667–I_672.

Laïbi, Raoul, Antoine, Gardel, Anthony, Edward J., Lucien-Marc, Oyede, 2012. Apport des sÉries d'images landsat dans l'Étude de la dynamique spatio-temporelle de l'embouchure de l'estuaire des fleuves mono et couffo au bÉnin, avant et aprÈs la construction du barrage de nangbÉto sur le mono. Teledetection, Editions des Archives Contemporaines, pp. 179–198.

Laïbi, Raoul A., Anthony, Edward J., Almar, Rafael, Castelle, Bruno, Senechal, Nadia, Kestenare, Elodie, 2014. Longshore drift cell development on the human-impacted bight of Benin sand barrier coast, west africa. J. Coast Res. 70 (10070), 78–83.

Pellerin Le Bas, Xavier, Levoy, Franck, Robin, Nicolas, Anthony, Edward J., 2022. The formation and morphodynamics of complex multihooked spits and the contribution of swash bars. Earth Surf. Process. Landforms 47 (1), 159–178.

Levoy, Franck, Monfort, Olivier, Anthony, Edward J., 2023. Multi-decadal shoreline mobility of a managed sandy tidal coast (normandy, France): behavioural variability in a context of sea-level rise and increasing storm intensity. Regional Stud. Mar. Sci. 62, 102973.

Lorenzo, F., Alonso, A., Pagés, J.L., 2007. Erosion and accretion of beach and spit systems in northwest Spain: a response to human activity. J. Coast Res. 23 (4), 834–845.

Marcel, JF Stive, Aarninkhof, Stefan GJ., Hamm, Luc, Hanson, Hans, Larson, Magnus, Wijnberg, Kathelijne M., Nicholls, Robert J., Capobianco, Michele, 2002. Variability of shore and shoreline evolution. Coast. Eng. 47 (2), 211–235.

Marcel, JF Stive, Van de Kreeke, J., Lam, Nghiem T., Tung, Tran T., Ranasinghe, Roshanka, 2009. Empirical Relationships between Inlet Cross-Section and Tidal Prism: A Review. Proceedings Of Coastal Dynamics 2009: Impacts of Human Activities on Dynamic Coastal Processes (With CD-ROM), pp. 1–10.

Masselink, Gerd, van Heteren, Sytze, 2014. Response of wave-dominated and mixed-energy barriers to storms. Mar. Geol. 352, 321–347.

Massuanganhe, E.A., Arnberg, W., 2008. Monitoring spit development in pomene, southern Mozambique, using landsat data. GeoEnviron. Landscape Evolution 100, 119–127. https://doi.org/10.2495/GEO080121.

Medina-Lopez, Encarni, 2020. Machine learning and the end of atmospheric corrections: a comparison between high-resolution sea surface salinity in coastal areas from top and bottom of atmosphere sentinel-2 imagery. Rem. Sens. 12 (18), 2924.

Melet, Angelique, Teatini, P., Le Cozannet, Gonéri, Jamet, C., Conversi, A., Benveniste, J., Almar, Rafael, 2020. Earth observations for monitoring marine coastal hazards and their drivers. Surv. Geophys. 41, 1489–1534.

Merritt, P Rice, 1974. Closure conditions mouth of the Russian river. Shore Beach 42 (1), 15–20.

Michel, Denis, Howa, H.L., 1997. Morphodynamic behaviour of a tidal inlet system in a mixed-energy environment. Phys. Chem. Earth 22 (3–4), 339–343.

Minh Duong, Trang, Ranasinghe, Roshanka, Luijendijk, Arjen, Walstra, DirkJan, Roelvink, Dano, 2017. Assessing climate change impacts on the stability of small tidal inlets: Part 1-data poor environments. Mar. Geol. 390, 331–346.

Murray Hicks, D., Hume, Terry M., Swales, Andrew, Magnitudes, Malcolm O Green, 1999. Spatial extent, time scales and causes of shoreline change adjacent to an ebb tidal delta, katikati inlet, New Zealand. J. Coast Res. 220–240.

Nahon, Alphonse, Idier, Déborah, Senechal, Nadia, Féniès, Hugues, Mallet, Cyril, Mugica, Julie, 2019. Imprints of wave climate and mean sea level variations in the dynamics of a coastal spit over the last 250 years: cap ferret, sw France. Earth Surf. Process. Landforms 44 (11), 2112–2125.

Ndour, Abdoulaye, Laïbi, Raoul A., Sadio, Mamadou, Degbe, Cossi G.E., Diaw, Amadou T., Oyédé, Lucien M., Anthony, Edward J., Dussouillez, Philippe, Sambou, Hyacinthe, Dièye, El hadji Balla, 2018. Management strategies for coastal erosion problems in west africa: analysis, issues, and constraints drawn from the examples of Senegal and Benin. Ocean Coast Manag. 156, 92–106. https://doi.org/10.1016/j.ocecoaman.2017.09.001. ISSN 0964-5691. https://www.sciencedirect.com/science/article/pii/S0964569117300728. SI: MSforCEP.

Nguyen, Quang Duc Anh, Tanaka, Hitoshi, Tam, Ho Sy, Tinh, Nguyen Xuan, Tung, Tran Thanh, Nguyen, Trung Viet, 2020. Comprehensive study of the sand spit evolution at tidal inlets in the central coast of vietnam. J. Mar. Sci. Eng. 8 (9) https://doi.org/10.3390/jmse8090722. ISSN 2077-1312.

Nicholas, C Kraus, Galgano, Francis A., 2001. Beach Erosional Hot Spots: Types, Causes, and Solutions. ENGINEER RESEARCH AND DEVELOPMENT CENTER VICKSBURG MS COASTAL AND HYDRAULICS LAB. Technical report.

Nicholas C Kraus, 1999. Analytical Model of Spit Evolution at Inlets. Technical Report, ARMY ENGINEER WATERWAYS EXPERIMENT STATION VICKSBURG MS COASTAL AND.

Palalane, Jaime, Larson, Magnus, Hanson, Hans, 2014. Analytical model of sand spit evolution. In: Proceedings of 34th International Conference on Coastal Engineering.

Pierce, J.W., 1969. Sediment budget along a barrier island chain. Sediment. Geol. 3 (1), 5–16.

Powell, Mark A., Thieke, Robert J., Mehta, Ashish J., 2006. Morphodynamic relationships for ebb and flood delta volumes at Florida's tidal entrances. Ocean Dynam. 56 (3), 295–307.

Pradhan, Umakanta, Mishra, Pravakar, Mohanty, Pratap Kumar, Behera, Balaji, 2015. Formation, growth and variability of sand spit at rushikulya river mouth, south odisha coast, India. Procedia Eng. 116, 963–970. https://doi.org/10.1016/j.proeng.2015.08.387. ISSN 1877-7058. https://www.sciencedirect.com/science/article/pii/S1877705815020421, 8th International Conference on Asian and Pacific Coasts (APAC 2015).

Ranasinghe, Roshanka, Pattiaratchi, Charitha, Masselink, Gerhard, 1999. A morphodynamic model to simulate the seasonal closure of tidal inlets. Coast. Eng. 37 (1), 1–36.

Robin, Nicolas, Levoy, Franck, Monfort, Olivier, 2007. Bar morphodynamic behaviour on the ebb delta of a macrotidal inlet (normandy, France). J. Coast Res. 23 (6), 1370–1378.

Robin, Nicolas, Levoy, Franck, Anthony, Edward J., Monfort, Olivier, 2020. Sand spit dynamics in a large tidal-range environment: insight from multiple lidar, uav and hydrodynamic measurements on multiple spit hook development, breaching, reconstruction, and shoreline changes. Earth Surf. Process. Landforms 45 (11), 2706–2726.

Sadio, Mamadou, Anthony, Edward J., Diaw, Amadou Tahirou, Dussouillez, Philippe, Fleury, Jules T., Kane, Alioune, Almar, Rafael, Kestenare, Elodie, 2017. Shoreline changes on the wave-influenced Senegal river delta, west africa: the roles of natural processes and human interventions. Water 9 (5). https://doi.org/10.3390/w9050357. ISSN 2073-4441.

Schmeltz, E.J., Sorensen, R.M., McCarthy, M.J., Nersesian, G., 1982. Breach/inlet interaction at moriches inlet. Coast. Eng. 1982 1062–1077.

Schoonees, J.S., Lenhoff, L., Raw, A.J., 1998. Preventing natural breaching of the major sand spit protecting the port of walvis bay. Coast. Eng 1999, 1475–1488.

Schwartz, Maurice L., 1982. The Encyclopedia of Beaches and Coastal Environments.

Stephen, P Leatherman, 1979. Migration of assateague island, Maryland, by inlet and overwash processes. Geology 7 (2), 104–107.

Taveneau, Adélaïde, Almar, Rafaël, Bergsma, Erwin W.J., Sy, Boubou Aldiouma, Ndour, Abdoulaye, Sadio, Mamadou, Garlan, Thierry, 2021. Observing and predicting coastal erosion at the langue de barbarie sand spit around saint louis (senegal, west africa) through satellite-derived digital elevation model and shoreline. Rem. Sens. 13 (13) https://doi.org/10.3390/rs13132454. ISSN 2072-4292. https://www.mdpi.com/2072-4292/13/13/2454.

Tran, Thanh Tung, Walstra, Dirk-Jan R., van de Graaff, Jan, Stive, Marcel JF., 2009. Morphological modeling of tidal inlet migration and closure. J. Coast Res. 1080–1084.

Tran, Thanh-Tung, Kreeke, Jacobus van de, Stive, Marcel JF., Walstra, Dirk-Jan R., 2012. Cross-sectional stability of tidal inlets: a comparison between numerical and empirical approaches. Coast. Eng. 60, 21–29.

Turner, Ian L., Harley, Mitchell D., Almar, Rafael, Bergsma, Erwin WJ., 2021. Satellite optical imagery in coastal engineering. Coast. Eng. 167, 103919.

Ty, V Wamsley, Kraus, Nicholas C., 2005. Coastal Barrier Island Breaching, Part 2: Mechanical Breaching and Breach Closure. Technical Report. ENGINEER RESEARCH AND DEVELOPMENT CENTER VICKSBURG MS COASTAL AND HYDRAULICSLAB.

Villagran, M.F., Cienfuegos, R., Almar, R., Catalán, P.A., Camaño, A., 2011. Natural post-tsunami recovery of the mataquito river mouth, after the 2010 chilean tsunami. AGU Fall Meeting Abstracts 2011. OS44B–05.

Vos, Kilian, Splinter, Kristen D., Harley, Mitchell D., Simmons, Joshua A., Coastsat, Ian L. Turner, 2019. A google earth engine-enabled python toolkit to extract shorelines from publicly available satellite imagery. Environ. Model. Software 122, 104528. https://doi.org/10.1016/j.envsoft.2019.104528. ISSN 1364-8152.

Zăinescu, Florin, Anthony, Edward, Vespremeanu-Stroe, Alfred, 2021. River jets versus wave-driven longshore currents at river mouths. Front. Mar. Sci. 8, 708258.

Zaremba, Robert E., Leatherman, Stephen P., 1984. Overwash processes and foredune ecology, nauset spit, Massachusetts. Technical report, Army Eng. Waterways Experiment Station Vicksburg Ms Environ. Lab.